Pharmaceutical Research, Vol. 22, No. 6, June 2005 (© 2005)
DOI: 10.1007/s11095-005-4576-1

Short Communication

Multidrug Resistance–Associated Protein 1 Functions as an Efflux Pump of Xenobiotics in the Skin

Qing Li,[1] Yukio Kato,[1] Yoshimichi Sai,[1] Teruko Imai,[2] and Akira Tsuji[1,3]

Received November 18, 2004; accepted February 23, 2005

Purpose. Recent research has identified gene expression of several types of xenobiotic transporters in the skin. The aim of this study was to investigate whether multidrug resistance–associated protein 1 (MRP1) functions in the skin.
Methods. The distribution of [^{14}C]grepafloxacin *in vivo* and the transport of 1-[2-amino-5-(2,7-dichloro-6-hydroxy-3-oxo-9-xanthenyl)phenoxy]-2-(2-amino-5-methylphenoxy)ethane-*N,N,N′,N′*-tetraacetic acid (fluo 3) were examined in the skin of Mrp1 knockout mice [FVB/Mrp1(−/−)] and normal mice [FVB/Mrp1(+/+)].
Results. The tissue-to-plasma concentration ratio of [^{14}C]grepafloxacin was higher in the skin of FVB/Mrp1(−/−) mice than that of FVB/Mrp1(+/+) mice. In skin slices of hairless mouse incubated with fluo 3 pentaacetoxymethyl ester, the accumulation of fluo 3 was significantly increased in the presence of probenecid (2 mM) and carbonyl cyanide *p*-trifluoromethoxyphenylhydrazone (5 μM) in a time-dependent manner but did not change in the presence of tetraethylammonium (2 mM). In FVB/Mrp1(−/−) mouse skin, the accumulation of fluo 3 increased time-dependently, while no increase was observed in FVB/Mrp1(+/+) mouse skin.
Conclusions. These findings suggest that Mrp1 is involved in the efflux of [^{14}C]grepafloxacin and fluo 3 in the skin, possibly acting as part of a barrier system against xenobiotic compounds.

KEY WORDS: confocal image; multidrug resistance–associated protein (MRP); skin.

INTRODUCTION

Skin is a dynamic organ having various defense mechanisms to protect the body from environmental factors; it acts not only as a physical barrier but also as a biochemical barrier. Constitutive expression of xenobiotic-metabolizing enzymes has been detected in normal human keratinocytes (1–3), in addition to the expression of glutathione *S*-transferase P1 (GSTP1) and GST activity (4). Recently, the expression of ATP-binding cassette transporters such as multidrug resistance–associated protein 1 (MRP1), MRP3, MRP4, MRP5, MRP6, and lung resistance protein (LRP) was also reported in normal human keratinocytes (3). The MRPs function as efflux transporters of glutathione *S*-conjugates (5,6). In addition, the expression of MRP1, the most highly expressed drug transporter in the skin, is increased, together with that of GSTP1 in lesional psoriatic skin treated with ultraviolet radiation (7). There has been no direct evidence that MRP1 functions in the efflux of drugs in the skin. Therefore, the aim of this study was to investigate whether MRP1 functions in the skin. Grepafloxacin, a fluoroquinolone, is a substrate of MRP1 (8) and is reported to have a weak photosensitizing action, like other fluoroquinolones (9). We examined the K_p values of [^{14}C]grepafloxacin in the skin of Mrp1 knockout mice [FVB/Mrp1(−/−)] and compared them with that of wild mice [FVB/Mrp1(+/+)]. Furthermore, confocal images of 1-[2-amino-5-(2,7-dichloro-6-hydroxy-3-oxo-9-xanthenyl) phenoxy]-2-(2-amino-5-methylphenoxy)ethane-*N,N,N′,N′*-tetraacetic acid (fluo 3) were obtained in skin slices from hairless mouse, and FVB/Mrp1(+/+) and FVB/Mrp1(−/−) mice preloaded with the fluo 3 precursor, fluo 3 pentaacetoxymethyl ester (fluo 3-AM). Fluo 3 is a fluorescent substrate of MRPs, while fluo 3-AM is a nonfluorescent ester that readily passes through cell membranes due to its lipophilic tail (10–13). After cleavage of the ester by cell-membrane esterases, hydrophilic fluo 3 is normally sequestered in the cytoplasm and excreted from the cells, possibly by efflux pump MRPs (10–13). Keratinoctyes were co-stained with *N*-(3-triethylammoniumpropyl)-4-(6-(4-(diethylamino)phenyl) hexatrienyl)pyridinium dibromide (FM4-64) to image the epidermal architecture. FM4-64 is a nontoxic, water-soluble dye that has no fluorescence in water but emits red fluorescence when inserted into membranes (14–16).

[1] Graduate School of Natural Science and Technology, Kanazawa University, Kakuma-machi, Kanazawa, Ishikawa, Japan.
[2] Faculty of Pharmaceutical Sciences, Kumamoto University, Kumamoto, Japan.
[3] To whom correspondence should be addressed. (e-mail: tsuji@kenroku.kanazawa-u.ac.jp)

MATERIALS AND METHODS

Materials

[^{14}C]grepafloxacin (81.2 μCi/mg) was kindly supplied by Otsuka Seiyaku Co., Ltd. (Tokyo, Japan). Fluo 3-AM and fluo 3 were purchased from Dojindo Laboratories (Tokyo, Japan). FM4-64 was purchased from Molecular Probes, Inc. (Eugene, OR, USA).

Animals

Five- to seven-week-old male hairless mice (HR-1) were purchased from Japan SLC (Hamamatsu, Japan). Five- to seven-week-old FVB/Mrp1(−/−) and FVB/Mrp1(+/+) mice were purchased from Taconic (Germantown, NY, USA) and CLEA Japan Inc. (Tokyo, Japan), respectively. Animal studies were performed in accordance with the Guidelines for the Care and Use of Laboratory Animals in Takaramachi Campus of Kanazawa University.

Distribution of [^{14}C]Grepafloxacin in the Tissues

[^{14}C]Grepafloxacin dissolved in 50 μl of saline was i.v. injected at a dose of 0.25 mg/kg. At 2 h after dosing, the mice were sacrificed under ether anesthesia and immediately dissected. The skin from the back and abdomen and the liver and the kidney were isolated, weighed, and solubilized in Soluene-350 at 50°C for 3 h. Radioactivity was measured by liquid scintillation counting. Tissue-to-plasma concentration ratio (K_p value) was evaluated using Eq. (1), where C_{tissue} and C_{plasma} represent concentration of grepafloxacin in the tissue and plasma, respectively. Statistical analysis was performed by the Student's *t* test. A difference between means was considered to be significant when the *p* value was less than 0.05.

$$K_p = \frac{C_{tissue}}{C_{plasma}} \quad (1)$$

Thin-layer chromatography (TLC) was performed to determine the parent compound, as described previously (17). Briefly, the skin sheets were solubilized in 1 N NaOH for 30 min, homogenized, mixed with three volumes of acetonitrile, and centrifuged to precipitate proteins. Aliquots of these supernatants were applied to TLC plates and developed with chloroform-methanol-28% ammonia (7:3:0.5, v/v/v). The profiles of radioactivity on the TLC plates were analyzed using a Typhoon9200 Variable Mode Imager (Amersham Biosciences). The recovery of [^{14}C]grepafloxacin was more than 72% in the skin and 90% in the plasma.

Confocal Microscope Method to Examine Export of Fluo 3

The slices of skin (100 μm) were sectioned with a microslicer (DTK-2000, Dosaka EM Co., Ltd. Kyoto, Japan) at 4°C. The slices were soaked in ice-cold Hanks' balanced salt solution (HBSS, 0.952 mM $CaCl_2$, 5.36 mM KCl, 0.441 mM KH_2PO_4, 0.812 mM $MgSO_4$, 136.7 mM NaCl, 0.385 mM Na_2HPO_4, 25 mM D-glucose, and 10 mM HEPES, pH 7.4) containing fluo 3-AM (10 μM) and FM4-64 (1 μlM) in the presence or absence of probenecid (2 mM), tetraethylammonium (TEA, 2 mM), or carbonyl cyanide *p*-trifluoromethoxyphenylhydrazone (FCCP, 5 μM) for 2 h. Then, the slices were placed on LabTek chambered cover glass and rapidly mounted on the stage of a confocal microscope at room temperature (20–22°C); this was taken as time 0. An inverted Zeiss Axiovert 100 M Laser Scanning Confocal Microscope 510 (LSM510) with a 63× water immersion objective lens was used to capture the confocal images. Lasers operating at 488 and 543 nm were used. A band pass filter for 505–530 nm was used to image fluo 3, and a 585-nm long-pass filter was used to image FM4-64. Serial confocal images were captured at room temperature.

Esterase Activity in the Skin

S9 fraction from skin homogenates (301.3 μg/ml) was prepared according to the method described previously (18). Hydrolysis experiments were initiated with 5 μM of fluo 3-AM after preincubating the homogenates (50 mM HEPES, 1 mM $CaCl_2$, pH 7.4) at 37°C for 5 min and loading various inhibitors at 37°C for 2 min. The velocity of the increase in fluorescence intensity of fluo 3 was measured during the first 9 min. No effect of calcium ion on the hydrolysis reaction in hairless mouse skin was apparent when *p*-nitrophenyl acetate was used as a substrate.

RESULTS AND DISCUSSION

FVB/Mrp1(−/−) mice were created by targeting in embryonic stem cells to disrupt Mrp1 gene (19,20). K_p value of [^{14}C]grepafloxacin in the skin of FVB/Mrp1(−/−) mice was significantly higher than that of FVB/Mrp1(+/+) mice (Table I). In agreement with a previous study (21), the K_p value of [^{14}C]grepafloxacin in the kidney of FVB/Mrp1(−/−) mice was significantly higher than that of FVB/Mrp1(+/+) mice, but no difference was observed in the K_p values in the liver between the two strains (Table I). Because the difference of K_p values between FVB/Mrp1(−/−) and FVB/Mrp1(+/+) mice was significant, but not remarkable, other transporter(s) most likely function(s) as an efflux transporter, too. According to the TLC method, more than 95% of the labeled compound was [^{14}C]grepafloxacin (data not shown). These results indicate that Mrp1 is involved in the efflux of [^{14}C]grepafloxacin in the skin *in vivo*.

Transporters expressed in the skin might play a role to kick-back the xenobiotics to the outside of the body. Based on the results of K_p values of grepafloxacin, however, it

Table I. Kp values of [^{14}C] grepafloxacin (μL/mg tissue)

	FVB/Mrp(+/+)[a]	FVB/Mrp(−/−)[b]	b/a
Skin	2.34 ± 0.01	2.83 ± 0.09*	1.21
Liver	10.77 ± 0.80	11.63 ± 0.29	1.08
Kidney	14.85 ± 1.09	18.40 ± 0.65*	1.24

Note: [^{14}C] Grepafloxacin (0.25 mg/kg) was administered i.v. to both types of mice. At 2 h after administration, plasma and skin associated radioactivities were quantitated. Each datum represents the mean ± SEM of 5 to 6 experiments.

* $P < 0.01$ *vs.* the FVB/ Mrp (+/+) mice.

might be possible that grepafloxacin was transported by MRP1 from the skin back to the blood, and further studies are needed to clarify the localization of MRP1 to demonstrate the direction of transport by MRP1 in the skin.

To clarify further the mechanism of MRP1 function in the skin, a fluorescent substrate of MRPs, fluo 3 was used. The confocal images were captured at room temperature (20–22°C), because fluo 3 is rapidly lost from keratinocytes at 37°C, resulting in difficulty in capturing fluorescent images. Bright and uniform fluorescence staining with FM4-64 in the membrane of keratinoctyes revealed a recognizable epidermal architecture from the stratum corneum (underpart) to the basal layer (upper) (Fig. 1). Time course for the fluorescence intensity of fluo 3 was then measured at room temperature. The fluorescence intensity of fluo 3 increased slowly in the presence of FCCP (5 μM), in a time-dependent manner, whereas no increase was observed without the inhibitor (data not shown). FCCP (5 μM) was widely used to investigate the effect as an ATP depressor. These results imply that fluo 3-AM was metabolized at room temperature in the keratinocytes and that the accumulation of fluo 3 in the keratinocytes was limited by an ATP-dependent efflux process. The accumulation of fluo 3 in the keratinocytes was remarkably increased in the presence of probenecid (a typical inhibitor of organic anion transporters) after 30 min but did not increase in the presence of TEA (a typical inhibitor of organic cationic transporters) or in the absence of any inhibitor (Fig. 1). These results suggested that an organic anion transport system(s), but not an organic cation transport system(s), was involved in the efflux of fluo 3 in the hairless mouse skin. The absence of any change in fluorescence intensity of FM4-64 under each condition suggested that the

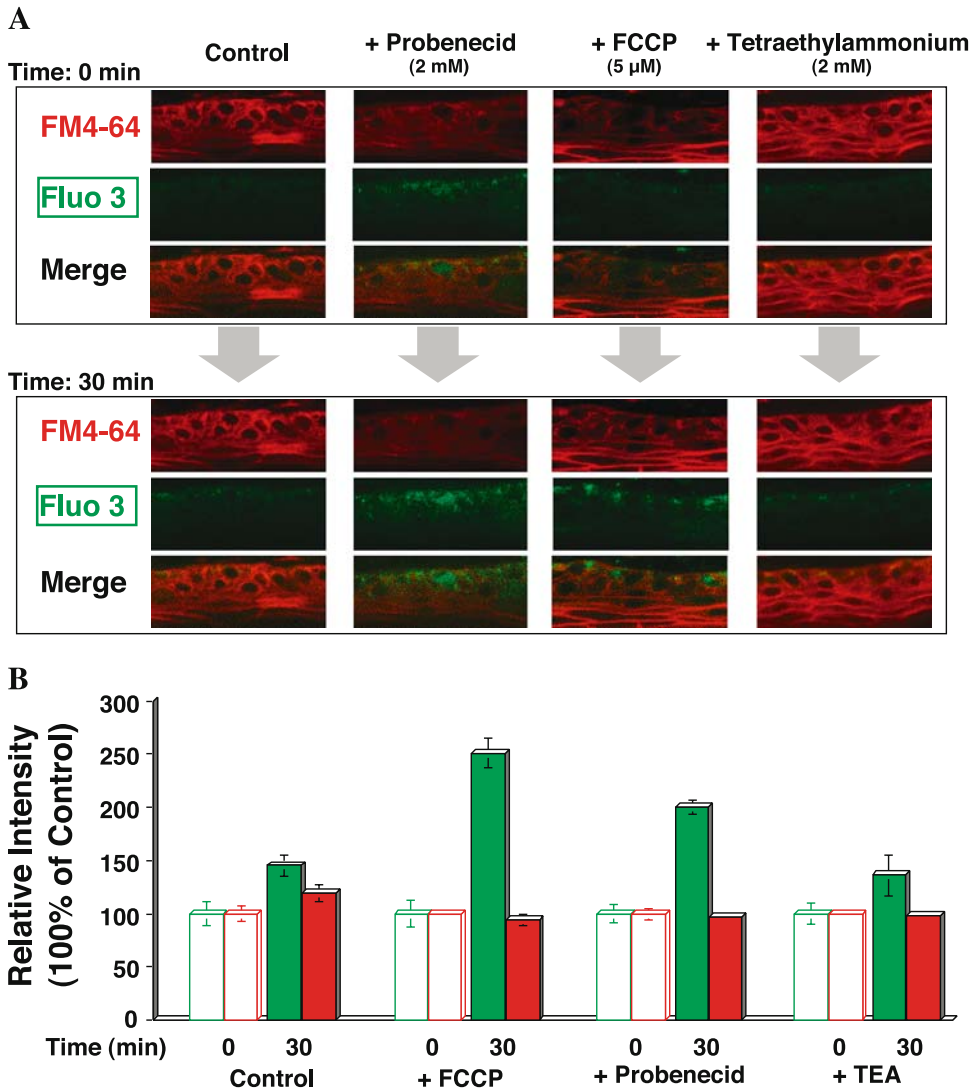

Fig. 1. Confocal images of fluo 3 in slices of hairless mouse skin at room temperature (20–22°C). Confocal images of fluo 3 in the presence or absence of various inhibitors, probenecid (2 mM), TEA (2 mM), and FCCP (5 μM), were also observed at 0 and 30 min (A). Based on these images, the relative average fluorescence intensities of fluo 3 and FM4-64 at 30 min (closed) in four locations were calculated, based on the intensity at 0 time (open) as 100% (B). Green and red columns represent the relative intensity of fluo 3 and FM4-64, respectively.

inhibitory effects were specific to fluo 3. In addition, TEA (89.1%) or FCCP (93.6%) had no significant effect on the activity of esterase in the skin (data not shown). Coadministration of probenecid (0.5 mM and 2 mM) inhibited the esterase activity to 64.9% and 59.4%, respectively (data not shown), so the increase in the accumulation of fluo 3 is not caused by an inhibitory effect on esterase activity in the skin but by an inhibitory effect on the efflux process of fluo 3 in the skin. Accumulation of fluo 3 in skin sections of FVB/Mrp1(−/−) mice was increased after 30 min, being similar to that observed in FVB/Mrp1(+/+) in the presence of probenecid, but in contrast to that in FVB/Mrp1(+/+) without the inhibitor (Fig. 2).

Fluo 3 is a fluorescent substrate for MRPs but is not specific for MRP1. However, in accordance with the results in the skin of hairless mice and Mrp1 knockout mice, these results indicate that Mrp1 is involved in the efflux of fluo 3 in the skin. Considering that probenecid inhibits organic anion transporters other than MRP1, further analysis should be performed to identify other transporters involved in dermal transport of fluo 3. Tight junctions of stratum granulosum were reported (22), but little information about the polarity

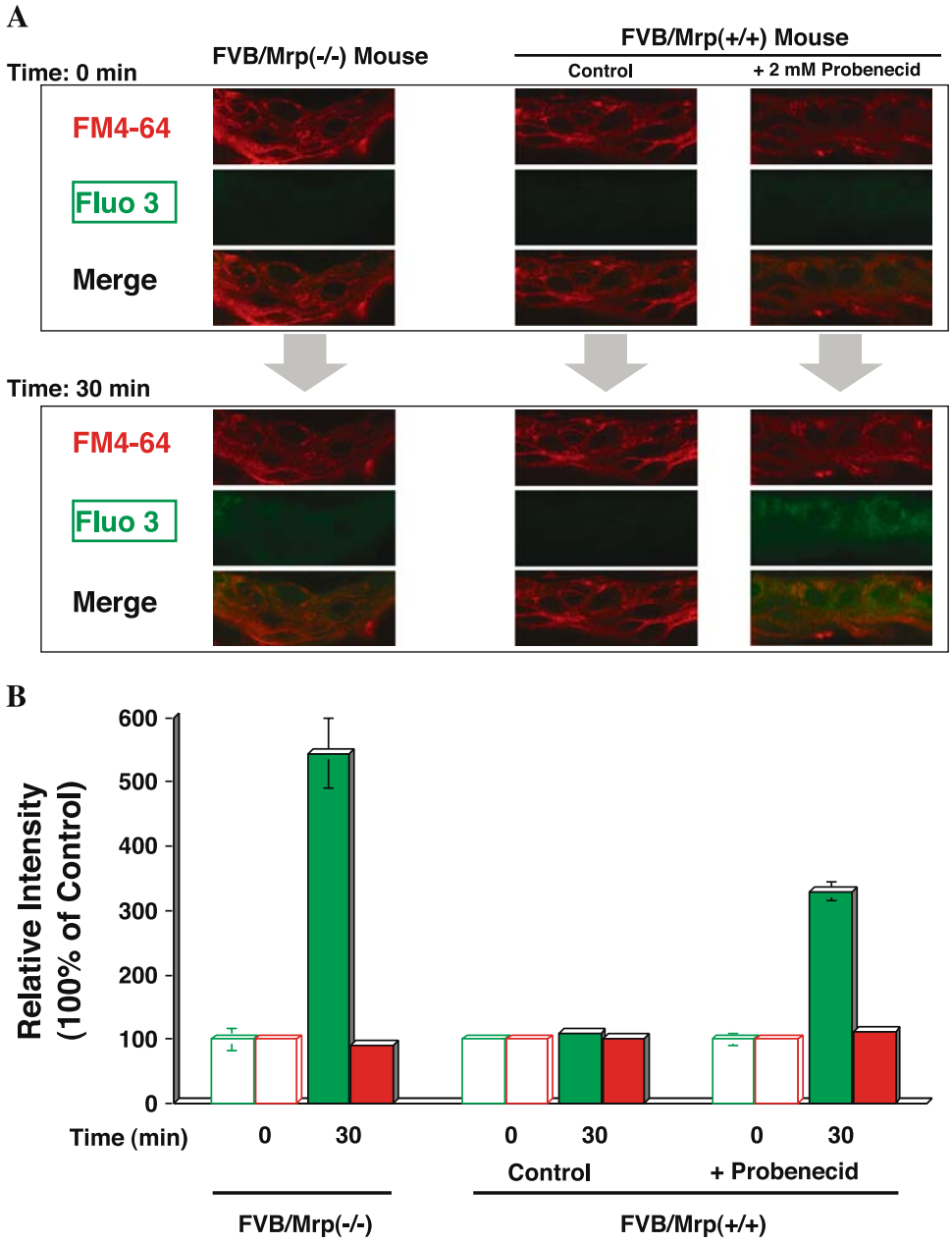

Fig. 2. Confocal images of fluo 3 in skin slices of FVBMrp1(+/+) and FVB/Mrp1(−/−) mice at room temperature (20–22°C). Confocal images of fluo 3 were captured at 0 and 30 min (A). Based on these images, the relative average fluorescence intensities of fluo 3 and FM4-64 at 30 min (closed) in four locations were calculated, based on the intensity at 0 time (open) as 100% (B). Green and red columns represent the relative intensity of fluo 3 and FM4-64, respectively.

of the keratinocytes is available. Further studies are needed to clarify the polarity of keratinocytes in order to characterize the physiologic role of the transporters.

In the current study, we show for the first time that MRP1 is involved in the efflux of [^{14}C]grepafloxacin in the skin. In the skin of healthy volunteers, the expression of MRP1 was the highest among various xenobiotic transporters examined, and it was increased in lesional psoriatic skin treated with ultraviolet radiation (7). Several single-nucleotide polymorphisms (SNPs) of MRP1 have been reported (23). MRP1 protein was detected in the membrane bound of keratinocytes by immunofluorescence (3), although the polarity of the membranes was not clarified. Therefore, it is possible that alterations in the regulation of MRP1 expression or different SNPs of MRP1 might be associated with changes in the efflux of xenobiotics in the keratinocytes and possibly with differences in the sensitizing effects of xenobiotics in the skin. Thus, MRP1 might be a novel target for improvement of drug delivery to the skin.

REFERENCES

1. F. K. Jugert, R. Agarwal, A. Kuhn, D. R. Bickers, H. F. Merk, and H. Mukhtar. Multiple cytochrome P450 isozymes in murine skin: induction of P450 1A, 2B, 2E, and 3A by dexamethasone. *J. Invest. Dermatol.* **102**:970–975 (1994).
2. D. S. Keeney, C. Skinner, J. B. Travers, J. H. Capdevila, L. B. Nanney, L. E. King Jr, and M. R. Waterman. Differentiating keratinocytes express a novel cytochrome P450 enzyme, CYP2B19, having arachidonate monooxygenase activity. *J. Biol. Chem.* **273**:32071–32079 (1998).
3. J. M. Baron, D. Holler, R. Schiffer, S. Frankenberg, M. Neis, H. F. Merk, and F. K. Jugert. Expression of multiple cytochrome p450 enzymes and multidrug resistance-associated transport proteins in human skin keratinocytes. *J. Invest. Dermatol.* **116**:541–548 (2001).
4. Y. Zhang, V. Gonzalez, and M. J. Xu. Expression and regulation of glutathione S-transferase P1-1 in cultured human epidermal cells. *J. Dermatol. Sci.* **30**:205–214 (2002).
5. T. Ishikawa. The ATP-dependent glutathione S-conjugate export pump. *Trends Biochem. Sci.* **17**:463–468 (1992).
6. G. J. Zaman, J. Lankelma, O. van Tellingen, J. Beijnen, H. Dekker, C. Paulusma, R. P. Oude Elferink, F. Baas, and P. Borst. Role of glutathione in the export of compounds from cells by the multidrug-resistance-associated protein. *Proc. Natl. Acad. Sci. USA* **92**:7690–7694 (1995).
7. G. Smith, R. S. Dawe, C. Clark, A. T. Evans, M. M. Comrie, C. R. Wolf, J. Ferguson, and S. H. Ibbotson. Quantitative real-time reverse transcription-polymerase chain reaction analysis of drug metabolizing and cytoprotective genes in psoriasis and regulation by ultraviolet radiation. *J. Invest. Dermatol.* **121**:390–398 (2003).
8. I. Tamai, J. Yamashita, Y. Kido, A. Ohnari, Y. Sai, Y. Shima, K. Naruhashi, S. Koizumi, and A. Tsugi. Limited distribution of new quinolone antibacterial agents into brain caused by multiple efflux transporters at the blood-brain barrier. *J. Pharmacol. Exp. Ther.* **295**:146–152 (2000).
9. J. Ferguson and R. Dawe. Phototoxicity in quinolones: comparison of ciprofloxacin and grepafloxacin. *J. Antimicrob. Chemother.* **40**:93–98 (1997).
10. T. H. Rushmore and C. B. Pickett. Glutathione S-transferases, structure, regulation, and therapeutic implications. *J. Biol. Chem.* **268**:11475–11478 (1993).
11. M. Lohoff, S. Prechtl, F. Sommer, M. Roellinghoff, E. Schmitt, G. Gradehandt, P. Rohwer, B. D. Stride, S. P. Cole, and R. G. Deeley. A multidrug-resistance protein (MRP)-like transmembrane pump is highly expressed by resting murine T helper (Th) 2, but not Th1 cells, and is induced to equal expression levels in Th1 and Th2 cells after antigenic stimulation *in vivo*. *J. Clin. Invest.* **101**:703–710 (1998).
12. A. T. Nies, T. Cantz, M. Brom, I. Leier, and D. Keppler. Expression of the apical conjugate export pump, Mrp2, in the polarized hepatoma cell line, WIF-B. *Hepatology* **28**:1332–1340 (1998).
13. D. Keppler, Y. Cui, J. Konig, I. Leier, and A. Nies. Export pumps for anionic conjugates. 8 encoded by MRP genes. *Adv. Enzyme Regul.* **39**:237–246 (1999).
14. S. L. Abrahamse and G. Rechkemmer. Identification of an organic anion transport system in the human colon carcinoma cell line HT29 clone 19A. *Pflugers. Arch.* **441**:529–537 (2001).
15. W. T. Godbey, K. K. Wu, and A. G. Mikos. Tracking the intracellular path of poly(ethyleneimine)/DNA complexes for gene delivery. *Proc. Natl. Acad. Sci. USA* **96**:5177–5181 (1999).
16. H. Pollard, J. S. Remy, G. Loussouarn, S. Demolombe, J. P. Behr, and D. Escande. Polyethylenimine but not cationic lipids promotes transgene delivery to the nucleus in mammalian cells. *J. Biol. Chem.* **273**:7507–7511 (1998).
17. H. Sasabe, A. Tsuji, and Y. Sugiyama. Carrier-mediated mechanism for the biliary excretion of the quinolone antibiotic grepafloxacin and its glucuronide in rats. *J. Pharmacol. Exp. Ther.* **284**:1033–1039 (1998).
18. S. Ahmed, T. Imai, Y. Yoshigae, and M. Otagiri. Stereospecific activity and nature of metabolizing esterases for propranolol prodrug in hairless mouse skin, liver and plasma. *Life Sci.* **61**:1879–1887 (1997).
19. J. Wijnholds, R. Evers, M. R. van Leusden, C. A. Mol, G. J. Zaman, U. Mayer, J. H. Beijnen, M. van der Valk, P. Krimpenfort, and P. Borst. Increased sensitivity to anticancer drugs and decreased inflammatory response in mice lacking the multidrug resistance-associated protein. *Nat. Med.* **3**:1275–1279 (1997).
20. J. Wijnholds, G. L. Scheffer, M. van der Valk, P. van der Valk, J. H. Beijnen, R. J. Scheper, and P. Borst. Multidrug resistance protein 1 protects the oropharyngeal mucosal layer and the testicular tubules against drug-induced damage. *J. Exp. Med.* **188**:797–808 (1998).
21. H. Sasabe, Y. Kato, T. Suzuki, M. Itose, G. Miyamoto, and Y. Sugiyama. Differential involvement of multidrug resistance-associated protein 1 and P-glycoprotein in tissue distribution and excretion of grepafloxacin in mice. *J. Pharmacol. Exp. Ther.* **310**:648–655 (2004).
22. M. Furuse, M. Hata, K. Furuse, Y. Yoshida, A. Haratake, Y. Sugitani, T. Noda, A. Kubo, and S. Tsukita. Claudin-based tight junctions are crucial for the mammalian epidermal barrier: a lesson from claudin-1-deficient mice. *J. Cell Biol.* **156:** 1099–1111 (2002).
23. S. Saito, A. Iida, A. Sekine, Y. Miura, C. Ogawa, S. Kawauchi, S. Higuchi, and Y. Nakamura. Identification of 779 genetic variations in eight genes encoding members of the ATP-binding cassette, subfamily C (ABCC/MRP/CFTR). *J. Hum. Genet.* **47**:147–171 (2002).